Research Paper

Neurovascular protection of alisol A on cerebral ischemia mice through activating the AKT/GSK3β pathway

Huihong Li[1,3,*], Caiyun Zhang[2,*], Yangjie Zhou[3], Yunfei Deng[3], Xiaoqing Zheng[3], Xiehua Xue[1,4]

[1]The Affiliated Rehabilitation Hospital, Fujian University of Traditional Chinese Medicine, Fuzhou, China
[2]The Zhangpu Hospital of Traditional Chinese Medicine, Zhangzhou, Fujian, China
[3]College of Rehabilitation Medicine, Fujian University of Traditional Chinese Medicine, Fuzhou, China
[4]Key Laboratory of Cognitive Rehabilitation of Fujian Province, Fuzhou, China
[*]Equal contribution and share first authorship

Correspondence to: Xiehua Xue; **email:** xuexiehua@aliyun.com, https://orcid.org/0000-0002-9018-1436
Keywords: alisol A, cerebral ischemia, hippocampus, neurovascular, AKT/GSK3β
Received: March 27, 2023 **Accepted:** October 2, 2023 **Published:** October 26, 2023

ABSTRACT

Alisol A, a triterpene isolated from Alisma Orientale, has been shown to exhibit anti-inflammatory effects and vascular protection. This study was designed to observe the effect of alisol A on cerebral ischemia (CI)-induced neurovascular dysfunction in the hippocampus and to further explore the potential mechanisms. The results showed that alisol A treatment improved the neurological deficits and cognitive impairment of CI mice. Alisol A reduced gliosis and improved neuronal/glial metabolism. Accordingly, alisol A inhibited inflammatory factors IL-6 and IL-1β induced by overactivation of astrocytes and microglia, thus protecting the neurovasculature. Furthermore, alisol A promoted the survival of neurons by decreasing the ratio of Bax/Bcl-2, and protected brain microvascular endothelial cells (BMECs) by upregulating the expression of ZO-1, Occludin and CD31. The phosphorylation of protein kinase B (AKT) and glycogen synthase kinase 3β (GSK3β) increased after treatment with alisol A. To explore the underlying mechanism, AKT was inhibited. As expected, the neurovascular protection of alisol A above was eliminated by AKT inhibition. The present study primarily suggested that alisol A could exert neurovascular protection in the hippocampus of CI mice by activating the AKT/GSK3β pathway and may potentially be used for the treatment of CI.

INTRODUCTION

Stroke is the third most common contributor to disability [1]. The incidence of CI accounts for approximately 87% of all stroke cases [2]. Stroke often leads to severe motor dysfunction and cognitive impairment. Cognitive impairment after stroke is highly prevalent (15%–70%) [3]. The prevalence of stroke increases during aging; therefore, CI occurs more often among elderly individuals. In recent years, stroke-related cognitive impairment has seriously endangered the health of the elderly [4]. Effective treatment of neurovascular dysfunction of CI has attracted increasing attention. The neurovascular function of the hippocampus plays an important role in the pathogenesis of CI [5]. CI induces inflammation, apoptosis, glial overactivation, blood brain barrier (BBB) and neuron disruption in the hippocampus, contributing to cognitive decline [6]. The neurovascular integrity in the hippocampus is critical for learning and memory and susceptible to ischemia and hypoxia [5]. Therefore, neurovascular protection in the hippocampus is extremely important for the treatment of CI.

AKT, a serine-threonine kinase, plays a vital role in cell death/survival. Phosphorylated/activated AKT is decreased in focal ischemia with aging [7]. Activated AKT exhibits a wide range of phosphorylation cascade

events and phosphorylates GSK3β. GSK3β plays a pivotal role in regulating the balance between pro-inflammatory and anti-inflammatory effects. GSK3β is inactivated by PI3K/AKT activation, which protects the brain by promoting angiogenesis, neurogenesis, anti-apoptosis, and anti-inflammation. Activation of the AKT/GSK3β signaling pathway enhanced neurovascular restoration against ischemic brain injury [8]. Furthermore, inhibition of AKT/GSK3β was involved in ischemia-induced cognitive impairment [9]. These findings suggest that the AKT/GSK3β pathway plays a key role in neurovascular protection and cognitive improvement.

Traditional Chinese medicine (TCM) has multiple targets for improving CI [10]. In recent years, the pharmacology of Alisma Orientale has attracted increasing attention. Alisma Orientale are used to treat cardiovascular diseases, inflammatory diseases, and prevent atherosclerosis [11]. Triterpenoids isolated from the dried rhizomes of Alisma species have been shown to have antiproliferative, antiallergic, antibacterial and antiviral properties [12]. Alisol A is one of the main single component extracts of Alisma Orientale and shows significant anti-inflammatory and anti-atherosclerosis effects. It has been reported that alisol A is a multitargeted agent that exerts vascular protection by inhibiting inflammation [13]. The protein-protein interaction network analysis showed that AKT is one of the core therapeutic targets of Alisma Orientale [14]. The PI3K/AKT pathway is the central mechanism of Alisma Orientale [12]. These findings suggest that AKT may be one of the key targets of alisol A in the treatment of CI-induced neurovascular destruction. Therefore, we speculated that alisol A might play a role in neurovascular protection and alleviate cognitive decline by activating the AKT/GSK3β pathway.

MATERIALS AND METHODS

Animals

C57BL/6J mice (n = 50) (male, weighing 22–25 g, 12 weeks) were obtained from GemPharmatech (Jiangsu, China). All procedures, protocols, treatments and sampling were approved by the Ethics Committee of Fujian University of Traditional Chinese Medicine and were performed in strict accordance with the animal care and use guidelines of the National Institutes of Health. Permit number: SCXK (Su) 2018-0008). Animal ethics approval number: 2020091. The CI model was produced as described previously [15]. Mice were anesthetized with 1% pentobarbital sodium (0.3 ml/100 g), and both carotid arteries were occluded for 20 minutes. Then, the occlusion was removed to restore cerebral blood flow. Mice in the sham group received the same surgical procedure, but the carotid arteries were not occluded.

Experimental design

Alisol A (Shanghai Yuanye Bio-Technology, Shanghai, China, B21638) was suspended in a solvent made up of lotus root powder and normal saline and then fully stirred in a warm bath to disperse evenly, and administered by gavage once a day for 7 consecutive days after CI (30 mg/kg). The AKT inhibitor GSK690693 (Apexbio, TX, USA, Catalog No. A5072) was injected intraperitoneally into mice at a dosage of 30 mg/kg [16] for 3 days and dissolved in DMSO. After CI, mice were randomly divided into four groups: sham-operated group (sham group, n = 10), cerebral ischemia group (CI group, n = 10), cerebral ischemia + alisol A group (CI+AA group, n = 10), and cerebral ischemia + alisol A+AKT inhibitor group (CI+AA+inh group, n = 10). The sham group and CI group were administered equal amounts of lotus root powder.

Modified neurological severity score (mNSS)

mNSS was used to assess animals' motor, sensory, balance, and reflex behaviors in each group (n = 10), which was performed by an investigator who was blinded to the grouping at 1, 3, 5, and 7 days after CI. mNSS scores ranged from 0 to 18 points. 0, no deficit; 1–6, mild deficit; 7–12, moderate deficit; 13–18, severe deficit.

Morris water maze (MWM)

MWM was performed after 7 days of intragastric intervention, when the body capacity and wound of the mice had recovered completely. The first stage was MWM training (1–4th day). Mice in each group (n = 10) were dropped into the water from four different quadrants to swim to the target platform that was set before. Escape latency and total distance (the time and distance required for mice to find the target platform) were recorded in the MWM training stage. Mice were required to stay on the platform for 15 s once they reached the target platform for more than 60 s. The second stage is the MWM test (the 5th day). The platform was removed, and swimming trajectories to reach the platform were captured. The number of target quadrant crossings and time spent in the quadrant were recorded in the MWM test stage.

New object recognition test (NORT)

The ability of mice to recognize new objects was evaluated by NORT. Each mouse was allowed to explore the open-field arena (40 × 40 × 40 cm) for

5 minutes without objects during the adaptation stage. 24 hours after habituation, two identical objects were placed on opposite corners, and mice were allowed to explore the two objects for 5 minutes. After 24 hours, one of the identical objects was replaced with a novel object, and mice were placed in the arena again to explore novel objects and familiar objects for 5 minutes. The discrimination ratio was calculated as the ratio of the number of explorations of the novel object to the number of explorations of the two identical objects. The movements of mice in the arena were recorded with a digital camera. The objects and the open-field arena were cleaned with 70% ethanol between each trial.

Magnetic resonance spectroscopy (MRS)

MRS provides information on neuronal/glial metabolism. The hippocampal CA1 area was selected as the region of interest, with a 1 mm × 1 mm × 1 mm size. MRS was acquired using a PRESS sequence, and the parameters of MRS were TR = 1500 ms, TE = 144 ms, number of averages = 256, and voxel = 5 mm × 4 mm × 4 mm. The reference values for each metabolite are as follows: N-acetyl aspartate (NAA): 2.02 ppm; creatine (Cr): 3.05 ppm; choline (Cho): 3.2 ppm; myo-inositol (MI): 3.56 ppm. Cr was used as an internal reference to calculate the relative levels of other metabolites. TOPSPIN (V3.1, Bruker Biospin, Ettlingen, Germany) of the MRI instrument was used to analyze related images and data.

Transmission electron microscopy (TEM)

TEM was used to detect changes in the neurovascular ultrastructure after CI. The hippocampal CA1 region was cut into 1 mm × 1 mm × 1 mm blocks and postfixed in 4% paraformaldehyde and 2.5% glutaraldehyde at 4°C. Samples were washed with phosphate buffer saline 3 times and then immersed in 1% osmium tetroxide in 0.1 M phosphate buffer for 2 hours at 4°C. Samples were cut into ultrathin sections and stained with 3% lead citrate. Then, TEM (Hitachi, HT7800, Tokyo, Japan) was used to observe and capture the neurovascular ultrastructure.

Nissl staining

After being fixed with 4% paraformaldehyde, tissues were embedded in paraffin and then cut into serial 4 μm-thick coronal sections. After dewaxing, the sections were stained with Nissl staining solution (Solarbio, cat# G1435, Beijing, China) for 30 min at 37°C. Subsequently, the sections were rinsed in graded ethanol and cleared with xylene. After drying thoroughly, the sections were cover slipped with neutral resin. Images were acquired with a Nikon microscope (Nikon, Model Eclipse Ci-L, 718345, Tokyo, Japan). The neuronal morphology of the hippocampal CA1 region was observed at 400X magnification. The number of surviving neurons was counted by ImageJ software (version 6.0; Motic China Group Co., Ltd., Xiamen, China) and calculated by averaging the number in the same fields of three sections. Three mice in each group were included in the statistical analysis.

Immunofluorescence staining

Immunofluorescence staining was applied to evaluate the expression of GFAP, Iba1, NeuN, and CD31 in the hippocampal CA1 region. Brain tissues were sliced into 4 μm-thick coronal sections and reacted with antibodies against GFAP (1:500, Proteintech, IL, USA, Cat No.: 16825-1-AP), Iba1 (1:500, Proteintech, Cat No.: 10904-1-AP), NeuN (1:500, Proteintech, Cat No.:26975-1-AP), and CD31 (1:500, Cell Signaling Technology, MA, USA) overnight at 4°C. The corresponding secondary antibodies of Alexa Fluor 594 (1:500, Cat# ab150080) were employed and reacted for 1 h. Then, DAPI was added (Beyotime, Shanghai, China, Cat No. P0131) before being photographed. Finally, images were captured using Leica Microsystems under a 200X microscope. The fluorescence intensity was analyzed according to previous literature [17] and measured in the ipsilateral hippocampal CA1 region by ImageJ software.

Western blot

The primary antibodies we used were as follows: ZO-1 (1:1000, Proteintech, Cat No. 21773-1-AP), Occludin (1:1000, Proteintech, Cat No. 66378-1-Ig), IL-6 (1:800, Proteintech, Cat. No. 66146-1-Ig), IL-1β (1:1000, Proteintech, Cat No. 16806-1-AP), BAX (1:1000, Proteintech, Cat No. 50599-2-Ig), Bcl-2 (1:1000, Proteintech, Cat No. 26593-1-AP), AKT (1:1000, Cell Signaling Technology, Cat#4691), P-AKT (Ser473, 1:1000, Cell Signaling Technology, Cat#4060), GSK3β (1:1000, Cell Signaling Technology, Cat# 12456S), P-GSK3β (1:1000, Cell Signaling Technology, Cat# 9323S), and GAPDH (1:8000, Proteintech, Cat# 60004-1-lg). The appropriate secondary antibodies (1:8000, Cat No. SA00001-1, Anti-Mouse; Cat No. SA00001-2 Anti-Rabbit) were incubated at room temperature for 1 hour. Finally, data were detected and analyzed by an Image Lab system (Bio-Rad, CA, USA, 721BR18682).

Statistical analysis

All statistical analyses were performed using SPSS 23.0. Data confirmed to have a normal distribution were analyzed by one-way ANOVA followed by the LSD or Games-Howell post hoc test and are presented as the mean ± SD. Values of $P < 0.05$ were considered statistically significant. Independent experiments were repeated at least 3 times.

RESULTS

Alisol A improved neurological deficits after CI

The molecular formula of alisol A is shown in Figure 1A. CI was established, and the detection of cerebral blood flow was described in a previous study [18]. The protective effects of alisol A against CI were examined by evaluating motor and sensory dysfunction according to mNSS (Figure 1B). Compared with the sham group, the CI group exhibited obvious neurological dysfunction. A significant improvement in mNSS was observed in mice treated with alisol A, while the result was reversed by the AKT inhibitor. The data above revealed that alisol A alleviated neurological deficits.

Alisol A improved cognitive impairment after CI

The learning and memory abilities of mice were evaluated by the MWM. The escape latency and total distance traveled showed a decreasing trend in the MWM training stage (Figure 1C, 1D). On Days 2–4 of the training stage, the escape latency of mice in the CI group was significantly prolonged ($P < 0.01$, $P < 0.001$, $P < 0.001$), and the total distance traveled was increased ($P < 0.01$, $P < 0.01$, $P < 0.01$) compared with the sham group. Compared with the CI group, alisol A treatment shortened the escape latency ($P < 0.001$, $P < 0.01$, $P < 0.01$) and decreased the total distance traveled ($P < 0.001$, $P < 0.01$, $P < 0.001$). Although the difference between the CI+AA group and the CI+AA+inh group was not significant on Days 1–3, it still indicated that the AKT inhibitor weakened the effect of alisol A on the spatial memory and learning abilities of mice. The differences in escape latency and total distance traveled were significant on Day 4 ($P < 0.001$, $P < 0.01$). On Day 5 of the test stage, compared with the sham group, there were significant reductions in the number of target platform crossings ($P < 0.001$) and time spent in the target quadrant ($P < 0.001$) in the CI group. The results were improved by the treatment of alisol A ($P < 0.001$, $P < 0.001$). However, the effect of alisol A was reversed by the AKT inhibitor ($P < 0.001$, $P < 0.001$) (Figure 1E, 1F). The trajectory diagram of mice in each group was significantly different in the number of target platform crossings (Figure 1H).

The recognition memory of mice was detected by NORT (Figure 1G). Compared with the sham group, the discrimination ratio in the CI group was significantly decreased ($P < 0.001$), increased in the CI+AA group ($P < 0.001$), and decreased in the CI+AA+inh group ($P < 0.001$). The trajectory diagram of the mice is shown in Figure 1I. The data above revealed that alisol A effectively alleviated cognitive impairment.

Alisol A regulated hippocampal metabolism

The relative levels of Cr, NAA, Cho and MI in the CA1 region of the hippocampus were detected by MRS (Figure 2A). Figure 2B shows a representative spectral image of the hippocampal CA1 region of mice. NAA is a specific biochemical marker to assess neuronal viability/integrity, and Cho and MI levels indicate information about glial metabolism [19]. The NAA/Cr ratio of the CI group was significantly reduced ($P < 0.05$), and the NAA/Cr ratio was increased by alisol A treatment ($P < 0.05$) and decreased by the AKT inhibitor ($P < 0.05$) (Figure 2C). The results indicated that alisol A treatment improved the destruction of neurons, while the effect was reversed by an AKT inhibitor. Compared with the sham group, Cho/Cr and MI/Cr ratios in the CI group increased with statistically significant ($P < 0.01$, $P < 0.01$). Alisol A decreased the ratios of Cho/Cr and MI/Cr ($P < 0.01$, $P < 0.01$), and the inhibitor reversed the results ($P < 0.05$, $P < 0.01$) (Figure 2D, 2E). MI and Cho have been considered putative glial markers, suggesting that alisol A reduced gliosis and improved neuronal/glial metabolism after CI.

Alisol A protected the neuronal ultrastructure in the hippocampal CA1 region

Neurons had an intact nuclear membrane structure and regular nuclear morphology in the sham group (Figure 3A (a, e)). Chromatin was distributed evenly within the nucleus. The nuclei with irregular shapes were slightly dissolved, and the chromatin showed condensation and edge aggregation and an incoherent nuclear membrane structure in the CI group (Figure 3A (b, f)). Moreover, some organelles were destroyed and even disappeared. The nuclear membrane was relatively intact, and the edge was clear after treatment with alisol A (Figure 3A (c, g)). In the inhibitor group (Figure 3A (d, h)), neurons with discontinuous and indistinct nuclear membrane structures had irregular morphology. Partial dissolution and disappearance of intracytoplasmic organelles can still be seen.

Alisol A protected the BBB ultrastructure in the hippocampal CA1 region

The sham group showed clear capillary brain structure, and the basal layer was in close contact with the endothelial cells and had a clear level of clarity (Figure 3B (a, e)). The CI group was characterized by discontinuity of the endothelium and TJs and swelling of the astrocytes (Figure 3B (b, f)). The capillary wall was thickened, and there was edema between the endothelial cells and basement membrane. Alisol A treatment improved the swelling of astrocyte end-feet,

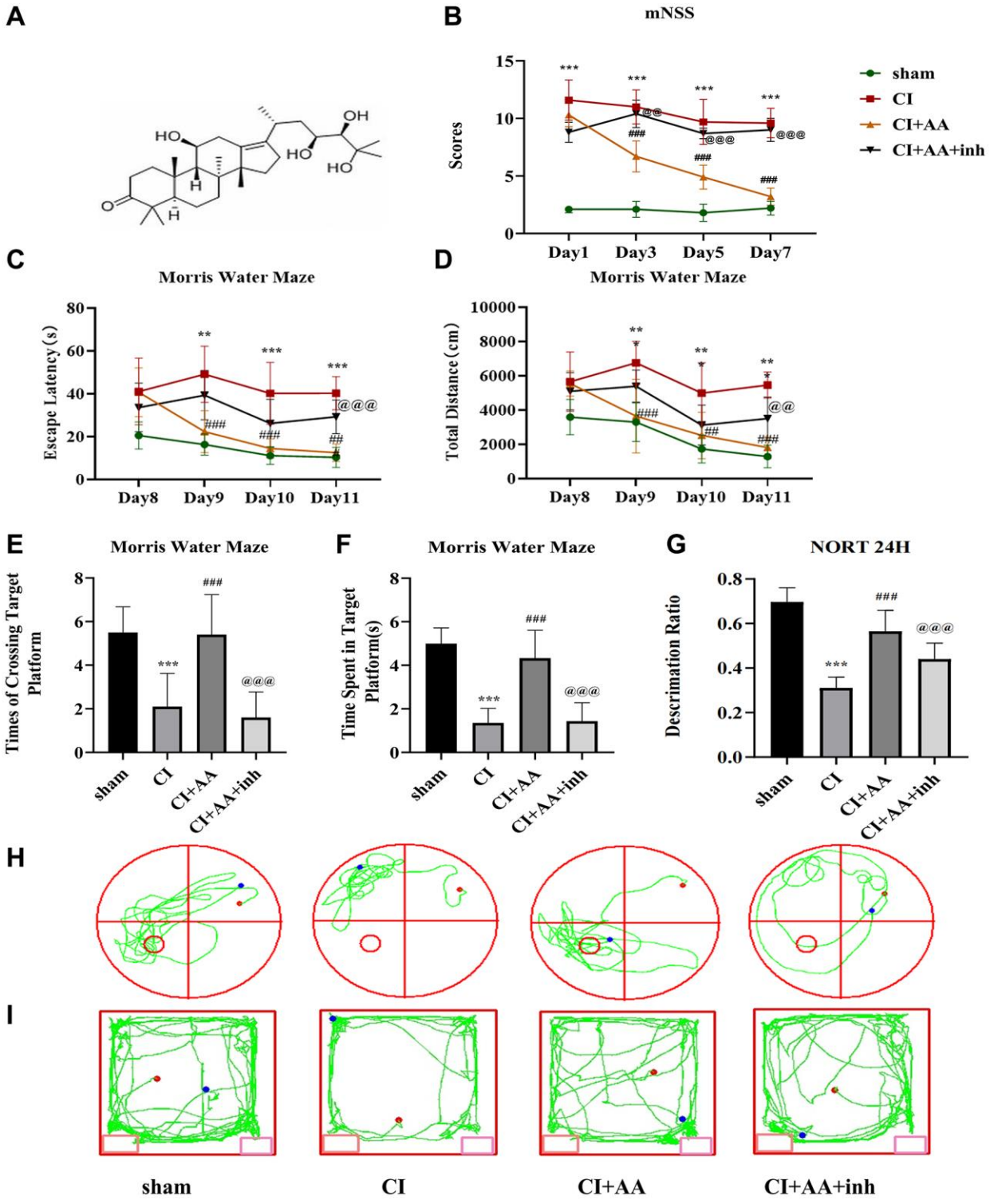

Figure 1. Alisol A improved neurological deficits and cognitive impairment after CI. (**A**) The molecular formula of alisol A. (**B**) Neurobehavioral function of mice was evaluated by mNSS at 1, 3, 5, and 7 days after CI, n = 10. (**C**) Escape latency of each group in the MWM training stage. (**D**) Total distance traveled by each group in the MWM training stage. (**E**) Frequency of crossing the target quadrant of each group in the MWM test. (**F**) Time spent in the target quadrant of each group in the MWM test. (**G**) Discrimination ratio of each group in NORT. (**H**) Representative tracking images in the MWM test. (**I**) Representative tracking images in NORT, n = 10. Data are shown as the mean ± SD. $^{**}P < 0.01$, $^{***}P < 0.001$ compared with the sham group, $^{\#\#}P < 0.01$, $^{\#\#\#}P < 0.001$ compared with the CI group, $^{@@}P < 0.01$, $^{@@@}P < 0.001$ compared with the CI+AA group. Note: sham-operated group (sham group); cerebral ischemia group (CI group); cerebral ischemia + alisol A (CI+AA group); cerebral ischemia + alisol A+AKT inhibitor group (CI+AA+inh group).

and the basal layer was in close contact with the endothelial cells, while there were still some vacuolar changes around the blood vessels (Figure 3B (c, g)). There was edema between the microvascular endothelial layer and basal lamina and discontinuity of the endothelium after inhibitor intervention (Figure 3B (d, h)).

Alisol A inhibited the expression of astrocytes, microglia, IL-6 and IL-1β after CI

The number of glial cells increased after CI, inducing inflammation in the brain. Astrocytes and microglia (Figure 4A, 4C) were overactivated in the CI group compared with the sham group ($P < 0.05$, $P < 0.05$). Alisol A inhibited the overexpression of GFAP and Iba1 ($P < 0.05$, $P < 0.05$), and the AKT inhibitor restored the overactivation of GFAP and Iba1 ($P < 0.01$, $P < 0.05$) (Figure 4B, 4D). Overactivated glial cells produce proinflammatory factors that further damage brain injury. The expression of IL-6 and IL-1β was increased in the CI group ($P < 0.01$, $P < 0.01$). Alisol A markedly reduced IL-6 and IL-1β levels ($P < 0.05$, $P < 0.05$). Compared with alisol A treatment, the AKT inhibitor increased the expression of IL-6 and IL-1β ($P < 0.05$, $P < 0.05$) (Figure 4E, 4F). The results revealed that alisol A inhibited glial activation and reduced the production of inflammatory factors.

Alisol A upregulated the expression of CD31, ZO-1 and Occludin after CI

CD31 is an angiogenesis marker that is mainly expressed in BMECs and is used to quantify the number of capillaries (Figure 5A). The expression of CD31 was decreased in the CI group ($P < 0.001$), alisol A treatment dramatically increased the expression of CD31 ($P < 0.05$), and the inhibitor abolished the effect of alisol A on CD31 expression ($P < 0.01$) (Figure 5B). ZO-1 and Occludin are important components of tight junction proteins (TJs), which are associated with BBB integrity and permeability. ZO-1 and Occludin were significantly decreased in the CI group ($P < 0.01$, $P < 0.001$), and alisol A treatment upregulated the expression of ZO-1 and Occludin ($P < 0.05$, $P < 0.05$), indicating that alisol A effectively protected the structure of the BBB by reducing the destruction of TJs. The AKT inhibitor reversed the effect of alisol A ($P < 0.01$, $P < 0.01$) (Figure 5C, 5D). The results confirmed that alisol A protected BMECs and TJs, which contributed to the protection of BBB integrity.

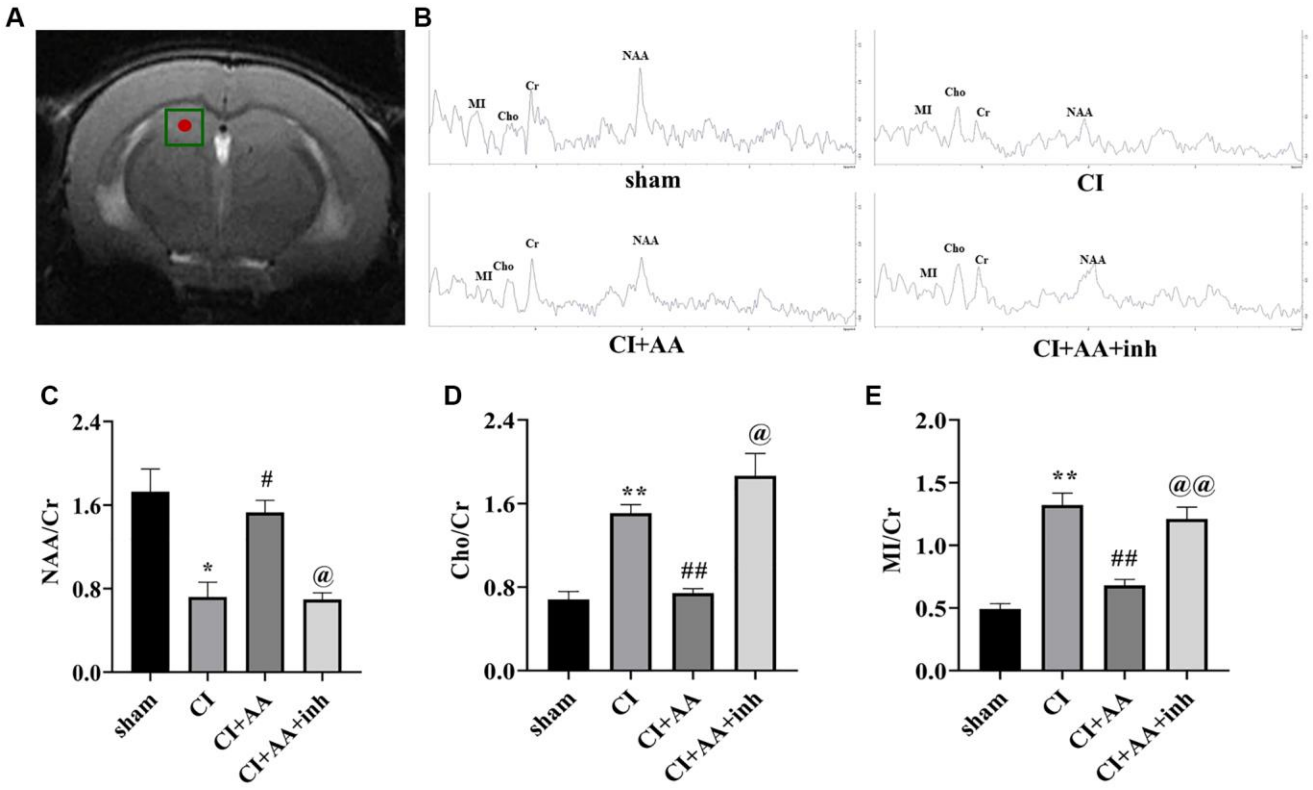

Figure 2. Alisol A regulated hippocampal metabolism. (**A**) The hippocampal CA1 region of mice was chosen as the region of interest. (**B**) Representative spectral image of the hippocampal CA1 region of mice. (**C**) Quantitative analysis of NAA/Cr. (**D**) Quantitative analysis of Cho/Cr. (**E**) Quantitative analysis of MI/Cr, $n = 6$. Data are presented as the mean ± SD, $^{*}P < 0.05$, $^{**}P < 0.01$ compared with the sham group, $^{\#}P < 0.05$, $^{\#\#}P < 0.01$ compared with the CI group, $^{@}P < 0.05$, $^{@@}P < 0.01$ compared with the CI+AA group.

Alisol A promoted neuronal survival in the hippocampus by downregulating the BAX/Bcl-2 ratio after CI

The expression of NeuN (Figure 6A) in the hippocampal CA1 region of the CI group was markedly decreased compared with that in the sham group ($P < 0.001$), while alisol A treatment increased the expression of NeuN ($P < 0.05$), and the inhibitor decreased the expression of NeuN ($P < 0.05$) (Figure 6B). Nissl staining was applied to detect surviving neurons in the hippocampal CA1 region (Figure 6C).

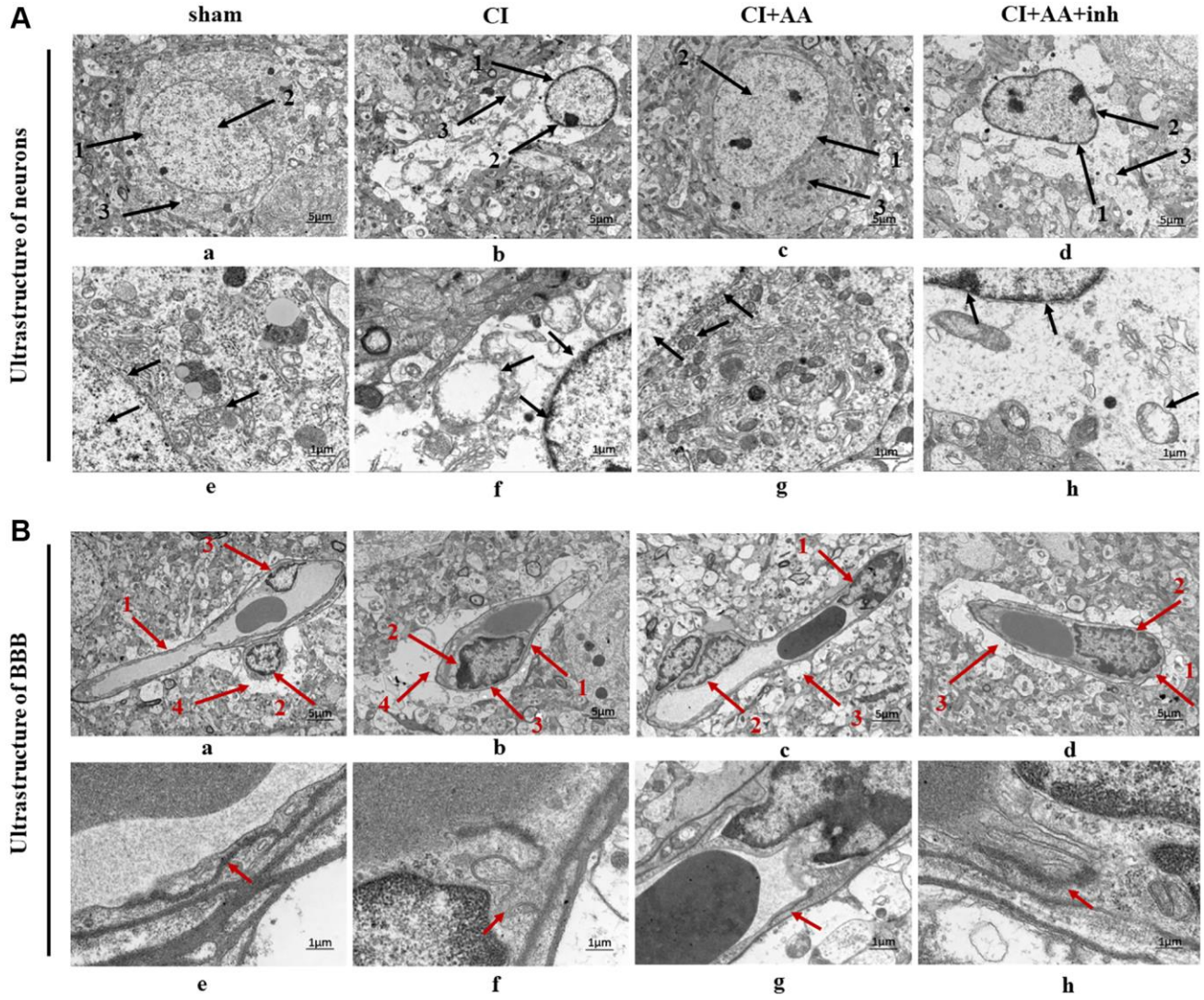

Figure 3. Alisol A protected the neurovascular ultrastructure in the hippocampal CA1 region. (**A**) Changes in neuronal ultrastructure are indicated by black arrows. (**a**) 1: The nuclear membrane structure of the neurons was intact and clear; 2: Chromatin distributed evenly; 3: Normal structural organelles were abundant within the cytoplasm. (**b**) 1: Incoherent nuclear membrane structure; 2: Chromatin condensation, decreased and edge aggregation; 3: Most of the organelles disappeared, and the cytoplasm was empty. (**c**) 1: The nuclear membrane is relatively complete, and the edge is clear; 2: More normal chromatin; 3: The organelles can be seen in the cytoplasm. (**d**) 1: Discontinuous and indistinct nuclear membrane structure; 2: Less chromatin; 3: Partial dissolution and disappearance of intracytoplasmic organelles. (**a**–**d**) Magnification of the microphotograph is 2500X. Scale bar is 5 μm; (**e**–**h**) Magnifications of the microphotograph are 8000X. Scale bar is 1 μm. (**B**) Changes in BBB ultrastructure as indicated by the red arrow. (**a**) 1: Clear capillary structures; 2: Close contact of the endothelial cells with the basement membrane; 3: Continuous endothelial cells; 4: End-feet of astrocyte surrounding the basal membrane. (**b**) 1: Capillary structure enhancement; 2: Edema fluid between the endothelial cells and the basement membrane; 3: Discontinuity of endothelium. 4: Marked edema of astrocytic end-foot processes and vacuolization. (**c**) 1: The edema between endothelial cells and the basal layer was weakened; 2: The endothelium was more continuous; 3: Vacuolization of astrocytic end-foot process edema was alleviated. (**d**) 1: There is edema between the endothelial cells and the basement membrane; 2: The endothelium is discontinuous and interrupted; 3: Perivascular astrocytic end-foot process edema was obvious and still showed vacuolar changes. (**a**–**d**) Magnification of the microphotograph is 2500X. Scale bar is 5 μm; (**e**–**h**) Magnifications of the microphotograph are 8000X. Scale bar is 1 μm. $n = 3$.

In the sham group, neuronal cells were arranged densely and neatly in the hippocampus. In contrast, the neuronal cells were arranged in a disorderly manner and even disappeared in the CI group ($P < 0.001$). Alisol A treatment restored the destruction of neurons during CI. The number of Nissl neurons in the alisol A group was higher than that in the CI group ($P < 0.001$) and inhibitor group ($P < 0.01$) (Figure 6D). Bcl-2 plays a role in promoting survival of neurons by inhibiting the expression of BAX. The BAX/Bcl-2 ratio in the CI group was higher than that in the sham group ($P < 0.01$), and the ratio in the alisol A group was lower than that in the CI group ($P < 0.05$) and AKT inhibitor group ($P < 0.05$) (Figure 6E). The results suggested that alisol A may promote neuronal survival in the CA1 region of the hippocampus by downregulating the BAX/Bcl-2 ratio.

Alisol A activated the AKT/GSK3β pathway after CI

To verify whether the AKT/GSK3β pathway is involved in the protective effects of alisol A, we detected the expression of phosphorylated AKT (Ser473) and GSK3β (Ser9). Phosphorylation of AKT and GSK3β was markedly decreased in the CI group ($P < 0.01$, $P < 0.05$). Alisol A promoted the phosphorylation of AKT and GSK3β ($P < 0.05$, $P < 0.05$). The phosphorylation levels of AKT and GSK3β were reversed following treatment with the AKT inhibitor ($P < 0.05$, $P < 0.05$) (Figure 6F, 6G). This result indicated that alisol A may exert protective effects on the neurovascular component of the hippocampus by activating the AKT/GSK3β pathway.

DISCUSSION

CI has seriously endangered the health of elderly individuals. The neurovascular integrity in the hippocampus is critical for learning and memory, which is susceptible to CI causes microglia-mediated inflammation and neurovascular disruption in the hippocampus, which is associated with cognitive impairment. Neurovascular impairment after CI primarily occurs in the hippocampal CA1 region and is often accompanied by cognitive impairment [20]. It is urgent to seek promising therapeutic strategies for neurovascular improvement with CI.

Alisma Orientale and its active constituents have been proven to have anti-inflammatory and vascular

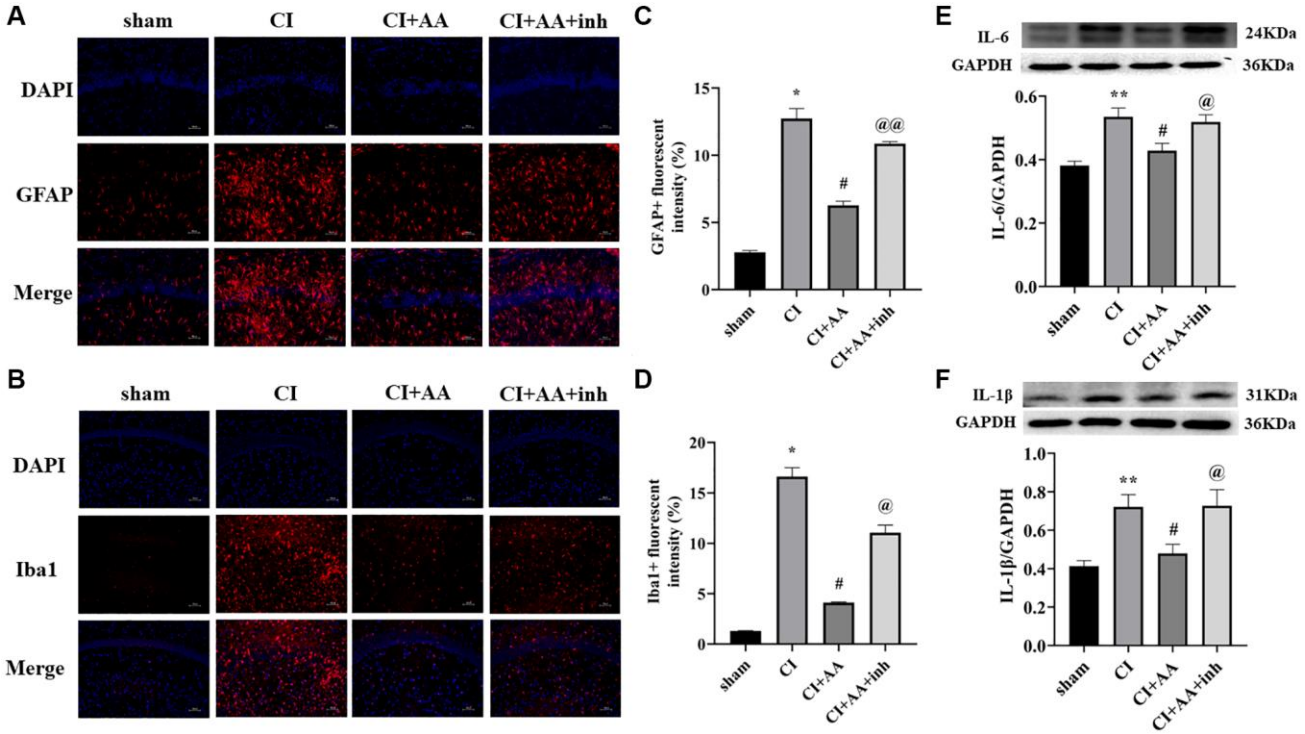

Figure 4. Alisol A inhibited the expression of astrocytes, microglia, IL-6 and IL-1β after CI. (**A**) Representative image of GFAP in the hippocampal CA1 region by immunofluorescence staining. (**B**) Representative image of Iba1 in the hippocampal CA1 region by using immunofluorescence staining. 200×, scale bar is 100 μm. (**C**) Quantitative analysis of GFAP fluorescence intensity. (**D**) Quantitative analysis of Iba1 fluorescence intensity, $n = 3$. (**E**) Western blot showing the expression of IL-6 and quantitative analysis of the ratio of IL-6 to GAPDH. (**F**) Western blot showing the expression of IL-1β and quantitative analysis of the ratio of IL-1β to GAPDH, $n = 4$. Data are shown as the mean ± SD. $^{*}P < 0.05$, $^{**}P < 0.01$ compared with the sham group, $^{\#}P < 0.05$ compared with the CI group, $^{@}P < 0.05$, $^{@@}P < 0.01$ compared with the CI+AA group.

protective effects and have been clinically used to treat cardiovascular-related diseases [21]. Alisol A, as the active ingredient isolated from Alisma Orientale, its effect on cerebrovascular diseases is rarely reported. It has been reported that alisol A exerted anti-obesity effect by ameliorating hyperlipidemia and inflammation state [22]. Alisol A could be detected in rat cerebral tissue after oral administration [23], indicating that alisol A could exert some effects on improving cerebrovascular diseases. Moreover, alisol A has been reported to exert vascular protection, attenuate the expression of proinflammatory cytokines, and increase the expression of phospho-AKT [24]. AKT is one of the core therapeutic targets of the mechanism of action of alisol A. Phospho-AKT exerts protective effects in CI by inactivating GSK3β [25]. AKT/GSK3β pathway is closely related to the inhibition of inflammation and apoptosis and the protection of vascular endothelium. Activation of AKT/GSK3β promotes neuronal survival in the hippocampus, reduces glial inflammation, and maintains BBB integrity after CI, demonstrating that the AKT/GSK3β pathway plays an important role in neurovascular protection [26]. We speculated that alisol A-mediated neurovascular protection might be

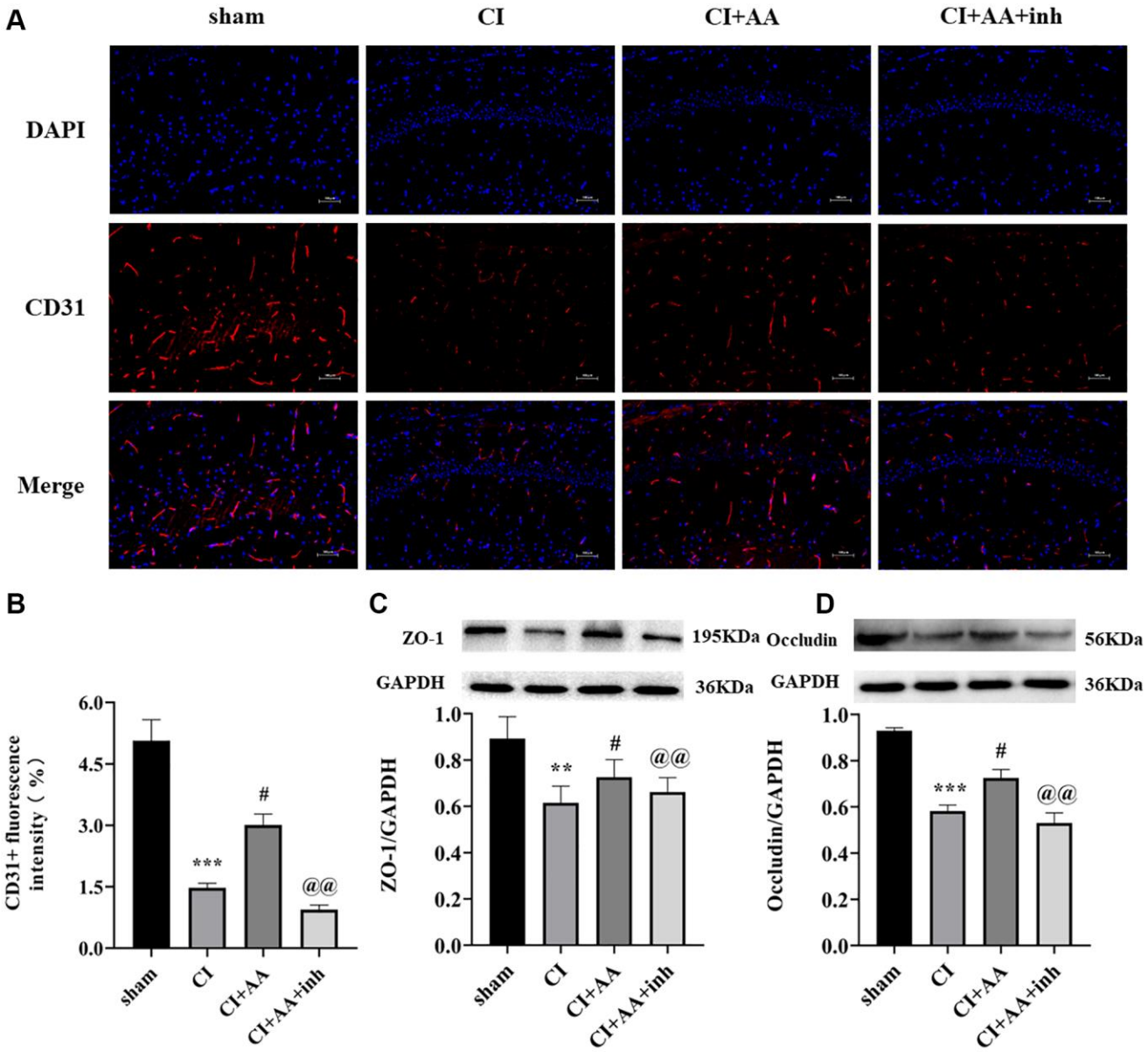

Figure 5. Alisol A upregulated the expression of CD31, ZO-1 and Occludin after CI. (**A**) Representative image of CD31 in the hippocampal CA1 region by using immunofluorescence staining. 200×, scale bar is 100 μm. (**B**) Quantitative analysis of CD31 fluorescence intensity. $n = 3$. (**C**) Western blot showing the expression of ZO-1 and quantitative analysis of the ratio of ZO-1 to GAPDH. (**D**) Western blot showing the expression of Occludin and quantitative analysis of the ratio of Occludin to GAPDH, $n = 4$. Data are shown as the mean ± SD. $^{**}P < 0.01$, $^{***}P < 0.001$ compared with the sham group, $^{\#}P < 0.05$ compared with the CI group, $^{@@}P < 0.01$ compared with the CI+AA group.

associated with the activation of AKT/GSK3β. The present study explored the neurovascular protection of alisol A, focusing on neurons, glial cells and BMECs. Our study is the first to show that alisol A has a protective effect on neurovasculature. We found that alisol A improved neurological deficits and cognitive impairment, inhibited glial activation, protected BMECs and TJs, promoted the survival of neurons and BMECs, and ameliorated neurovascular disruption in the hippocampus. Moreover, an AKT inhibitor reversed the protective effects of alisol A, which suggested that activation of the AKT/GSK3β pathway may participate in the neurovascular protection of alisol A.

MRS has been used to detect metabolic information in CI [27]. We first observed changes in neuronal loss and glial activation following ischemia according to the changes in NAA, Cho and MI levels, which may be associated with neurovascular dysfunction. Decreased NAA has been identified as a strong signal for neuronal loss [28]. The Cho concentration in glial cells is higher than that in neurons and may be used as a marker of gliosis [19]. MI is also a marker of glial proliferation [29]. Both Cho and MI levels increased after ischemia, indicating overactivation of glia after ischemia. Interestingly, AKT is a crucial regulator of cell energy metabolism, including cholinergic function, neurochemical differentiation, neuroprotection and inhibition of gliosis [30]. It was confirmed that activation of AKT regulated the levels of MI, Cho and NAA [18]. In this study, we found that CI induced the upregulation of Cho and MI and the downregulation of NAA. Interestingly, alisol A decreased Cho and MI concentrations in the hippocampal CA1 region while increasing the level of NAA, and an AKT inhibitor reversed this tendency. The results indicated that the regulatory effect of alisol A on hippocampal neuronal/glial metabolism might be related to the AKT/GKS3β pathway.

TEM results showed that the neurovascular ultrastructure was destroyed after CI, which manifested as neuronal morphological destruction, thickened capillary wall edema, and swelling of astrocytic end-foot processes in the hippocampus, which was consistent with a previous study [31]. Swollen astrocytic end-foot processes and perivascular edema are involved in the pathological process of BBB breakdown [32]. As expected, we found that treatment with alisol A improved the nuclear membrane of

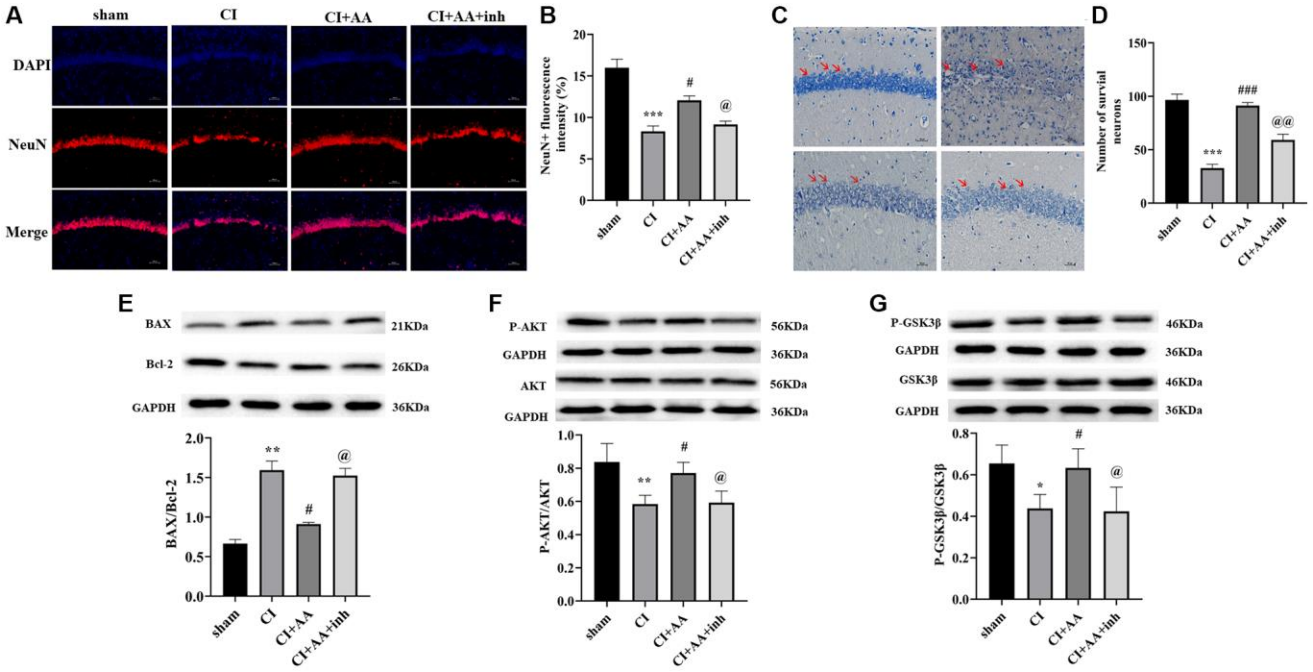

Figure 6. Alisol A reduced neuronal apoptosis in the hippocampus by downregulating the BAX/Bcl-2 ratio and activating the AKT/GSK3β pathway after CI. (**A**) Representative image of NeuN in the hippocampal CA1 region by using immunofluorescence staining. 200×, scale bar is 100 μm. (**B**) Quantitative analysis of NeuN fluorescence intensity, n = 3. (**C**) The neuronal morphology of the hippocampal CA1 region was observed by Nissl staining. 400×, scale bar is 50 μm. Red arrows show the morphology of neurons in different groups. (**D**) Quantitative analysis of intact neuronal cells in the hippocampal CA1 region, n = 3. (**E**) Western blot showing the expression of BAX and Bcl-2 and quantitative analysis of the BAX/Bcl-2 ratio. (**F**) Western blot showing the expression of p-AKT and AKT and quantitative analysis of the ratio of p-AKT to AKT. (**G**) Western blot showing the expression of p-GSK3β and GSK3β and quantitative analysis of the ratio of p-GSK3β to GSK3β, n = 4. Data are shown as the mean ± SD. $^{*}P < 0.05$, $^{**}P < 0.01$, $^{***}P < 0.001$ compared with the sham group, $^{\#}P < 0.05$, $^{\#\#\#}P < 0.001$ compared with the CI group, $^{@}P < 0.05$, $^{@@}P < 0.01$ compared with the CI+AA group.

neurons, mitochondrial cristae, swelling of astrocyte end-feet and endothelial cells, while the neurovascular protective effect was eliminated by an AKT inhibitor.

We further investigated the underlying mechanism of neurovascular changes. Microglia and astrocytes are overactivated after CI, inducing inflammatory dysfunction [33]. Reactive astrogliosis produces large amounts of proinflammatory factors and damages neurovascular homeostasis [34]. Microglia-mediated inflammation affects basal lamina integrity and leads to increased permeability of the BBB, ultimately resulting in significant neurovascular disruption [35]. A previous study showed that the activation of AKT/GSK3β inhibited the proinflammatory "M1" phenotype of microglia and then downregulated IL-6, IL-1β and TNF-α levels [36–38]. The present study showed that alisol A significantly inhibited the expression of GFAP and Iba1 and reduced the overactivation of glial cells. In addition, the levels of the inflammatory factors IL-6 and IL-1β also decreased after alisol A intervention. However, the effects of alisol A could be attenuated by inhibition of AKT at the same time, further confirming that the AKT/GSK3β pathway was involved in the anti-inflammatory effect of alisol A.

The release of inflammatory cytokines induced by over-activated glial cells has been demonstrated to further damage the BBB [39]. CD31 (an angiogenesis marker), mostly expressed in BMECs, plays a pivotal role in protecting BBB integrity [40]. The activation of the AKT/GSK3β pathway exerted an angiogenic effect, and raised the CD31 positive microvessel number, while the inhibition of AKT inhibited angiogenesis, which was consistent with our study [41]. In addition, TJs form a virtually impermeable barrier between BMECs, which is relevant in maintaining BBB integrity. Studies have indicated that activation of AKT/GSK3β reduces the disruption of ZO-1, Occludin and Claudin-5 by downregulating the expression of inflammatory factors [42]. In our study, alisol A treatment upregulated the expression of CD31, ZO-1 and Occludin and promoted vascular and endothelial protection in the hippocampus, whereas the effects were attenuated by an AKT inhibitor, further revealing that alisol A may protect the BBB through regulation of the AKT/GSK3β pathway.

Overactivated glial cells also aggravate neuronal apoptosis in the hippocampal CA1 region after CI [43]. In our study, NeuN immunofluorescence and Nissl staining showed that alisol A treatment promoted neuronal survival in the hippocampus after CI. In addition, we found that alisol A decreased the ratio of BAX/Bcl-2, which may be what promotes neuron survival. The effect of alisol A was eliminated by inhibition of AKT. Therefore, we further explored the underlying mechanism. Bcl-2 promotes neuronal survival by inhibiting the expression of the pro-apoptotic factor BAX [44], while BAX is involved in neuronal apoptosis by triggering mitochondrial dysfunction [45]. AKT inhibits inflammation and apoptosis by inactivating GSK3β, and GSK3β promotes translocation of this proapoptotic protein to mitochondria in neurons undergoing apoptosis by directly phosphorylating BAX on Ser163 [46]. The BAX/Bcl-2 ratio is increased by downregulating the phosphorylation levels of AKT and GSK3β [47]. Furthermore, activating the AKT/GSK3β pathway has been proven to mediate the survival of hippocampal CA1 neurons after CI [48]. Therefore, the results suggest that alisol A may promote the protective effect of alisol A on neuronal survival in the hippocampus and decrease the BAX/Bcl-2 ratio by activating the AKT/GSK3β pathway.

The AKT/GSK3β pathway plays an important role in the protective effects of alisol A on neurons and the BBB. Notably, the inhibition of AKT decreased the phosphorylation level of GSK3β and almost reversed the neurovascular protective effects of alisol A, which was consistent with our hypothesis. Our study is the first to show that alisol A has a protective effect on cerebrovascular. The present study also showed that AKT/GSK3β pathway was involved in the neuro-vascular protective effect of alisol A, which is another novelty different from other studies.

In conclusion, this study showed that alisol A alleviated neurovascular injury, which was mainly attributed to the activation of the AKT/GSK3β pathway by raising the phosphorylation of AKT and GSK3β.

CONCLUSIONS

Alisol A could exert an important role in neurovascular protection and alleviate cognitive impairment through activation of the AKT/GSK3β pathway in CI mice.

Abbreviations

CI: Cerebral Ischemia; BMECs: Brain Microvascular Endothelial Cells; GSK3β: Glycogen Synthase Kinase 3β; BBB: Blood Brain Barrier; TCM: Traditional Chinese Medicine; mNSS: Modified Neurological Severity Score; MWM: Morris Water Maze; NORT: New Object Recognition Test; MRS: Magnetic Resonance Spectroscopy; TEM: Transmission Electron Microscope; NAA: N-acetyl aspartate; Cr: Creatine; Cho: Choline; MI: Myo-inositol; TJs: Tight Junction Proteins.

AUTHOR CONTRIBUTIONS

H.L. (Huihong Li) designed the study and wrote the manuscript. C.Z. (Caiyun Zhang) performed the animal behavior test. Y.Z. (Yangjie Zhou) performed the experiments. Y.D. (Yunfei Deng) and X.Z. (Xiaoqing Zheng) collected and analyzed the data. X.X. (Xiehua Xue) revised the manuscript. All authors read and approved the final manuscript.

ACKNOWLEDGMENTS

We are most grateful to Institute of Rehabilitation Industry and Key Laboratory of Rehabilitation Technology of Fujian Province.

CONFLICTS OF INTEREST

The authors declare no conflicts of interest related to this study.

ETHICAL STATEMENT

All procedures, protocols, treatments and sampling were approved by the Ethics Committee of Fujian University of Traditional Chinese Medicine and were performed in strict accordance with the animal care and use guidelines of the National Institutes of Health. Permit number: SCXK (Su) 2018-0008). Animal ethics approval number: 2020091.

FUNDING

This work was supported by the National Natural Science Foundation of China (Grant Number 82274620), the Natural Science Foundation of Fujian Province, China (Grant Number 2021zyyj69) and (Grant Number 2021J01957).

REFERENCES

1. Ghozy S, Reda A, Varney J, Elhawary AS, Shah J, Murry K, Sobeeh MG, Nayak SS, Azzam AY, Brinjikji W, Kadirvel R, Kallmes DF. Neuroprotection in Acute Ischemic Stroke: A Battle Against the Biology of Nature. Front Neurol. 2022; 13:870141. https://doi.org/10.3389/fneur.2022.870141 PMID:35711268

2. Wang L, Liu Y, Zhang X, Ye Y, Xiong X, Zhang S, Gu L, Jian Z, Wang H. Endoplasmic Reticulum Stress and the Unfolded Protein Response in Cerebral Ischemia/Reperfusion Injury. Front Cell Neurosci. 2022; 16:864426. https://doi.org/10.3389/fncel.2022.864426 PMID:35602556

3. Rost NS, Meschia JF, Gottesman R, Wruck L, Helmer K, Greenberg SM, and DISCOVERY Investigators. Cognitive Impairment and Dementia After Stroke: Design and Rationale for the DISCOVERY Study. Stroke. 2021; 52:e499–516. https://doi.org/10.1161/STROKEAHA.120.031611 PMID:34039035

4. Kanamaru T, Suda S, Muraga K, Ishiwata A, Aoki J, Suzuki K, Sakamoto Y, Katano T, Nishimura T, Nishiyama Y, Kimura K. Pre-stroke cognitive impairment in acute ischemic stroke patients predicts poor functional outcome after mechanical thrombectomy. Neurol Sci. 2021; 42:4629–35. https://doi.org/10.1007/s10072-021-05158-6 PMID:33666769

5. Hatayama K, Riddick S, Awa F, Chen X, Virgintino D, Stonestreet BS. Time Course of Changes in the Neurovascular Unit after Hypoxic-Ischemic Injury in Neonatal Rats. Int J Mol Sci. 2022; 23:1945. https://doi.org/10.3390/ijms23084180 PMID:35456999

6. Liu M, Xu Z, Wang L, Zhang L, Liu Y, Cao J, Fu Q, Liu Y, Li H, Lou J, Hou W, Mi W, Ma Y. Cottonseed oil alleviates ischemic stroke injury by inhibiting the inflammatory activation of microglia and astrocyte. J Neuroinflammation. 2020; 17:270. https://doi.org/10.1186/s12974-020-01946-7 PMID:32917229

7. Du X, Yang J, Liu C, Wang S, Zhang C, Zhao H, Du H, Geng X. Hypoxia-Inducible Factor 1α and 2α Have Beneficial Effects in Remote Ischemic Preconditioning Against Stroke by Modulating Inflammatory Responses in Aged Rats. Front Aging Neurosci. 2020; 12:54. https://doi.org/10.3389/fnagi.2020.00054 PMID:32210788

8. Li MZ, Zhang Y, Zou HY, Ouyang JY, Zhan Y, Yang L, Cheng BC, Wang L, Zhang QX, Lei JF, Zhao YY, Zhao H. Investigation of Ginkgo biloba extract (EGb 761) promotes neurovascular restoration and axonal remodeling after embolic stroke in rat using magnetic resonance imaging and histopathological analysis. Biomed Pharmacother. 2018; 103:989–1001. https://doi.org/10.1016/j.biopha.2018.04.125 PMID:29710516

9. Chen B, Zhang M, Ji M, Zhang D, Chen B, Gong W, Li X, Zhou Y, Dong C, Wen G, Zhan X, Wu X, Yuan H, et al. The neuroprotective mechanism of lithium after ischaemic stroke. Commun Biol. 2022; 5:105. https://doi.org/10.1038/s42003-022-03051-2 PMID:35115638

10. Bai X, Zhang M. Traditional Chinese Medicine Intervenes in Vascular Dementia: Traditional

Medicine Brings New Expectations. Front Pharmacol. 2021; 12:689625. https://doi.org/10.3389/fphar.2021.689625 PMID:34194332

11. Wang H, Wang H, Zhang J, Luo J, Peng C, Tong X, Chen X. Molecular Mechanism of Crataegi Folium and Alisma Rhizoma in the Treatment of Dyslipidemia Based on Network Pharmacology and Molecular Docking. Evid Based Complement Alternat Med. 2022; 2022:4891370. https://doi.org/10.1155/2022/4891370 PMID:35722157

12. Bailly C. Pharmacological Properties and Molecular Targets of Alisol Triterpenoids from Alismatis Rhizoma. Biomedicines. 2022; 10:1945. https://doi.org/10.3390/biomedicines10081945 PMID:36009492

13. Wang K, Zhang B, Song D, Xi J, Hao W, Yuan J, Gao C, Cui Z, Cheng Z. Alisol A Alleviates Arterial Plaque by Activating AMPK/SIRT1 Signaling Pathway in apoE-Deficient Mice. Front Pharmacol. 2020; 11:580073. https://doi.org/10.3389/fphar.2020.580073 PMID:33224034

14. Liao Y, Ding Y, Yu L, Xiang C, Yang M. Exploring the mechanism of Alisma orientale for the treatment of pregnancy induced hypertension and potential hepato-nephrotoxicity by using network pharmacology, network toxicology, molecular docking and molecular dynamics simulation. Front Pharmacol. 2022; 13:1027112. https://doi.org/10.3389/fphar.2022.1027112 PMID:36457705

15. Wang J, Bai T, Wang N, Li H, Guo X. Neuroprotective potential of imatinib in global ischemia-reperfusion-induced cerebral injury: possible role of Janus-activated kinase 2/signal transducer and activator of transcription 3 and connexin 43. Korean J Physiol Pharmacol. 2020; 24:11–8. https://doi.org/10.4196/kjpp.2020.24.1.11 PMID:31908570

16. Sun L, Cui K, Xing F, Liu X. Akt dependent adult hippocampal neurogenesis regulates the behavioral improvement of treadmill running to mice model of post-traumatic stress disorder. Behav Brain Res. 2020; 379:112375. https://doi.org/10.1016/j.bbr.2019.112375 PMID:31759046

17. Song Z, Feng J, Zhang Q, Deng S, Yu D, Zhang Y, Li T. Tanshinone IIA Protects Against Cerebral Ischemia Reperfusion Injury by Regulating Microglial Activation and Polarization via NF-κB Pathway. Front Pharmacol. 2021; 12:641848. https://doi.org/10.3389/fphar.2021.641848 PMID:33953677

18. Lu T, Li H, Zhou Y, Wei W, Ding L, Zhan Z, Liu W, Tao J, Xue X. Neuroprotective effects of alisol A 24-acetate on cerebral ischaemia-reperfusion injury are mediated by regulating the PI3K/AKT pathway. J Neuroinflammation. 2022; 19:37. https://doi.org/10.1186/s12974-022-02392-3 PMID:35130910

19. Han H, Xiao JH, Weng Y, Liang H, Han C, Yi C, Lin K, Wu H. Evidence of persistent glial cell dysfunction in the anterior cingulate cortex of juvenile idiopathic arthritis children: a proton MRS study. Pediatr Rheumatol Online J. 2022; 20:53. https://doi.org/10.1186/s12969-022-00711-9 PMID:35897107

20. Ward R, Valenzuela JP, Li W, Dong G, Fagan SC, Ergul A. Poststroke cognitive impairment and hippocampal neurovascular remodeling: the impact of diabetes and sex. Am J Physiol Heart Circ Physiol. 2018; 315:H1402–13. https://doi.org/10.1152/ajpheart.00390.2018 PMID:30118341

21. Wu Y, Wang X, Yang L, Kang S, Yan G, Han Y, Fang H, Sun H. Therapeutic Effects of Alisma orientale and its Active Constituents on Cardiovascular Disease and Obesity. Am J Chin Med. 2023; 51:623–50. https://doi.org/10.1142/S0192415X23500301 PMID:36961296

22. Ho C, Gao Y, Zheng D, Liu Y, Shan S, Fang B, Zhao Y, Song D, Zhang Y, Li Q. Alisol A attenuates high-fat-diet-induced obesity and metabolic disorders via the AMPK/ACC/SREBP-1c pathway. J Cell Mol Med. 2019; 23:5108–18. https://doi.org/10.1111/jcmm.14380 PMID:31144451

23. Xu W, Li X, Lin N, Zhang X, Huang X, Wu T, Tai Y, Chen S, Wu CH, Huang M, Wu S. Pharmacokinetics and tissue distribution of five major triterpenoids after oral administration of Rhizoma Alismatis extract to rats using ultra high-performance liquid chromatography-tandem mass spectrometry. J Pharm Biomed Anal. 2017; 146:314–23. https://doi.org/10.1016/j.jpba.2017.09.009 PMID:28910706

24. Jia XK, Huang JF, Huang XQ, Li XY, Huang MQ, Zhu HC, Li GP, Lan ML, Yu ZW, Xu W, Wu SS. Alismatis Rhizoma Triterpenes Alleviate High-Fat Diet-Induced Insulin Resistance in Skeletal Muscle of Mice. Evid Based Complement Alternat Med. 2021; 2021:8857687. https://doi.org/10.1155/2021/8857687 PMID:33623531

25. Wang HJ, Ran HF, Yin Y, Xu XG, Jiang BX, Yu SQ, Chen YJ, Ren HJ, Feng S, Zhang JF, Chen Y, Xue Q, Xu XY. Catalpol improves impaired neurovascular unit in ischemic stroke rats via enhancing VEGF-PI3K/AKT and VEGF-MEK1/2/ERK1/2 signaling. Acta Pharmacol Sin. 2022; 43:1670–85. https://doi.org/10.1038/s41401-021-00803-4 PMID:34795412

26. Jin B, Kim H, Choi JI, Bae HB, Jeong S. Avenanthramide C Prevents Neuronal Apoptosis via PI3K/Akt/GSK3β Signaling Pathway Following Middle Cerebral Artery Occlusion. Brain Sci. 2020; 10:878. https://doi.org/10.3390/brainsci10110878 PMID:33233587

27. Wang R, Hu B, Sun C, Geng D, Lin J, Li Y. Metabolic abnormality in acute stroke-like lesion and its relationship with focal cerebral blood flow in patients with MELAS: Evidence from proton MR spectroscopy and arterial spin labeling. Mitochondrion. 2021; 59:276–82. https://doi.org/10.1016/j.mito.2021.06.012 PMID:34186261

28. Mazibuko N, Tuura RO, Sztriha L, O'Daly O, Barker GJ, Williams SCR, O'Sullivan M, Kalra L. Subacute Changes in N-Acetylaspartate (NAA) Following Ischemic Stroke: A Serial MR Spectroscopy Pilot Study. Diagnostics (Basel). 2020; 10:482. https://doi.org/10.3390/diagnostics10070482 PMID:32708540

29. Brkic S, Veres B, Thurnher MM, Boban J, Radovanovic B, Tomic S, Kozic D. CNS efficacy parameters of combination antiretroviral therapy in chronic HIV infection: A multi-voxel magnetic resonance spectroscopy study. Front Neurol. 2023; 14:943183. https://doi.org/10.3389/fneur.2023.943183 PMID:37034085

30. Li T, Li J, Li T, Zhao Y, Ke H, Wang S, Liu D, Wang Z. L-Cysteine Provides Neuroprotection of Hypoxia-Ischemia Injury in Neonatal Mice via a PI3K/Akt-Dependent Mechanism. Drug Des Devel Ther. 2021; 15:517–29. https://doi.org/10.2147/DDDT.S293025 PMID:33603342

31. Feng XF, Li MC, Lin ZY, Li MZ, Lu Y, Zhuang YM, Lei JF, Wang L, Zhao H. Tetramethylpyrazine promotes stroke recovery by inducing the restoration of neurovascular unit and transformation of A1/A2 reactive astrocytes. Front Cell Neurosci. 2023; 17:1125412. https://doi.org/10.3389/fncel.2023.1125412 PMID:37051111

32. Huang J, Ding J, Wang X, Gu C, He Y, Li Y, Fan H, Xie Q, Qi X, Wang Z, Qiu P. Transfer of neuron-derived α-synuclein to astrocytes induces neuroinflammation and blood-brain barrier damage after methamphetamine exposure: Involving the regulation of nuclear receptor-associated protein 1. Brain Behav Immun. 2022; 106:247–61. https://doi.org/10.1016/j.bbi.2022.09.002 PMID:36089218

33. Zhang S, Zhang Y, Liu H, Wu F, Wang Z, Li L, Huang H, Qiu S, Li Y. Enriched environment remodels the central immune environment and improves the prognosis of acute ischemic stroke in elderly mice with chronic ischemia. Front Immunol. 2023; 14:1114596. https://doi.org/10.3389/fimmu.2023.1114596 PMID:36969204

34. Bandyopadhyay S. Role of Neuron and Glia in Alzheimer's Disease and Associated Vascular Dysfunction. Front Aging Neurosci. 2021; 13:653334. https://doi.org/10.3389/fnagi.2021.653334 PMID:34211387

35. Zhao Y, Wei ZZ, Lee JH, Gu X, Sun J, Dix TA, Wei L, Yu SP. Pharmacological hypothermia induced neurovascular protection after severe stroke of transient middle cerebral artery occlusion in mice. Exp Neurol. 2020; 325:113133. https://doi.org/10.1016/j.expneurol.2019.113133 PMID:31770520

36. Zu HB, Liu XY, Yao K. DHCR24 overexpression modulates microglia polarization and inflammatory response via Akt/GSK3β signaling in $A\beta_{25-35}$) treated BV-2 cells. Life Sci. 2020; 260:118470. https://doi.org/10.1016/j.lfs.2020.118470 PMID:32950573

37. Ramírez-Sánchez J, Pires ENS, Meneghetti A, Hansel G, Nuñez-Figueredo Y, Pardo-Andreu GL, Ochoa-Rodríguez E, Verdecia-Reyes Y, Delgado-Hernández R, Salbego C, Souza DO. JM-20 Treatment After MCAO Reduced Astrocyte Reactivity and Neuronal Death on Peri-infarct Regions of the Rat Brain. Mol Neurobiol. 2019; 56:502–12. https://doi.org/10.1007/s12035-018-1087-8 PMID:29725905

38. Zheng X, Cai X, Ye F, Li Y, Wang Q, Zuo Z, Huang W, Wang Z. Perioperative Dexmedetomidine attenuates brain ischemia reperfusion injury possibly via up-regulation of astrocyte Connexin 43. BMC Anesthesiol. 2020; 20:299. https://doi.org/10.1186/s12871-020-01211-7 PMID:33287729

39. Haruwaka K, Ikegami A, Tachibana Y, Ohno N, Konishi H, Hashimoto A, Matsumoto M, Kato D, Ono R, Kiyama H, Moorhouse AJ, Nabekura J, Wake H. Dual microglia effects on blood brain barrier permeability

induced by systemic inflammation. Nat Commun. 2019; 10:5816.
https://doi.org/10.1038/s41467-019-13812-z
PMID:31862977

40. Du J, Yin G, Hu Y, Shi S, Jiang J, Song X, Zhang Z, Wei Z, Tang C, Lyu H. Coicis semen protects against focal cerebral ischemia-reperfusion injury by inhibiting oxidative stress and promoting angiogenesis via the TGFβ/ALK1/Smad1/5 signaling pathway. Aging (Albany NY). 2020; 13:877–93.
https://doi.org/10.18632/aging.202194
PMID:33290255

41. Fei Y, Zhao B, Zhu J, Fang W, Li Y. XQ-1H promotes cerebral angiogenesis via activating PI3K/Akt/GSK3β/β-catenin/VEGF signal in mice exposed to cerebral ischemic injury. Life Sci. 2021; 272:119234.
https://doi.org/10.1016/j.lfs.2021.119234
PMID:33607158

42. Li L, Cheng SQ, Guo W, Cai ZY, Sun YQ, Huang XX, Yang J, Ji J, Chen YY, Dong YF, Cheng H, Sun XL. Oridonin prevents oxidative stress-induced endothelial injury via promoting Nrf-2 pathway in ischaemic stroke. J Cell Mol Med. 2021; 25:9753–66.
https://doi.org/10.1111/jcmm.16923
PMID:34514714

43. Khastar H, Garmabi B, Zare Mehrjerdi F, Rahimi MT, Shamsaei N, Ali AH, Khorsand N, Khaksari M. Cyanocobalamin improves memory impairment via inhibition of necrosis and apoptosis of hippocampal cell death after transient global ischemia/reperfusion. Iran J Basic Med Sci. 2021; 24:160–6.
https://doi.org/10.22038/IJBMS.2020.48447.11126
PMID:33953854

44. Zhang Y, Guo X, Wang G, Liu J, Liang P, Wang H, Zhu C, Wu Q. Effects of rhodioloside on the neurological functions of rats with total cerebral ischemia/reperfusion and cone neuron injury in the hippocampal CA1 region. PeerJ. 2020; 8:e10056.
https://doi.org/10.7717/peerj.10056
PMID:33240590

45. Wu Q, Mao Z, Liu J, Huang J, Wang N. Ligustilide Attenuates Ischemia Reperfusion-Induced Hippocampal Neuronal Apoptosis via Activating the PI3K/Akt Pathway. Front Pharmacol. 2020; 11:979.
https://doi.org/10.3389/fphar.2020.00979
PMID:32676033

46. Linseman DA, Butts BD, Precht TA, Phelps RA, Le SS, Laessig TA, Bouchard RJ, Florez-McClure ML, Heidenreich KA. Glycogen synthase kinase-3beta phosphorylates Bax and promotes its mitochondrial localization during neuronal apoptosis. J Neurosci. 2004; 24:9993–10002.
https://doi.org/10.1523/JNEUROSCI.2057-04.2004
PMID:15525785

47. Cai C, Wu Y, Yang L, Xiang Y, Zhu N, Zhao H, Hu W, Lv L, Zeng C. Sodium Selenite Attenuates Balloon Injury-Induced and Monocrotaline-Induced Vascular Remodeling in Rats. Front Pharmacol. 2021; 12:618493.
https://doi.org/10.3389/fphar.2021.618493
PMID:33790787

48. Park JH, Lee TK, Kim DW, Sim H, Lee JC, Kim JD, Ahn JH, Lee CH, Kim YM, Won MH, Choi SY. Neuroprotective Effects of Salicin in a Gerbil Model of Transient Forebrain Ischemia by Attenuating Oxidative Stress and Activating PI3K/Akt/GSK3β Pathway. Antioxidants (Basel). 2021; 10:629.
https://doi.org/10.3390/antiox10040629
PMID:33924188